



# Development of a Post-vitrectomy Injection of N-methyl-N-nitrosourea as a Localized Retinal Degeneration Rabbit Model

So Min Ahn<sup>1</sup>, Jungryul Ahn<sup>2</sup>, Seongkwang Cha<sup>2</sup>, Cheolmin Yun<sup>1</sup>,  
Tae Kwann Park<sup>3</sup>, Yong Sook Goo<sup>2\*</sup> and Seong-Woo Kim<sup>1\*</sup>

<sup>1</sup>Department of Ophthalmology, Korea University College of Medicine, Seoul 08373,

<sup>2</sup>Department of Physiology, Chungbuk National University School of Medicine, Cheongju 28644,

<sup>3</sup>Department of Ophthalmology, Soonchunhyang University Hospital Bucheon, Bucheon 14584, Korea

Since genetic models for retinal degeneration (RD) in animals larger than rodents have not been firmly established to date, we sought in the present study to develop a new rabbit model of drug-induced RD. First, intravitreal injection of N-methyl-N-nitrosourea (MNU) without vitrectomy in rabbits was performed with different doses. One month after injection, morphological changes in the retinas were identified with ultra-wide-field color fundus photography (FP) and fundus autofluorescence (AF) imaging as well as spectral-domain optical coherence tomography (OCT). Notably, the degree of RD was not consistently correlated with MNU dose. Then, to check the effects of vitrectomy on MNU-induced RD, the intravitreal injection of MNU after vitrectomy in rabbits was also performed with different doses. In OCT, while there were no significant changes in the retinas for injections up to 0.1 mg (i.e., sham, 0.05 mg, and 0.1 mg), outer retinal atrophy and retinal atrophy of the whole layer were observed with MNU injections of 0.3 mg and 0.5 mg, respectively. With this outcome, 0.2 mg MNU was chosen to be injected into rabbit eyes (n=10) at two weeks after vitrectomy for further study. Six weeks after injection, morphological identification with FP, AF, OCT, and histology clearly showed localized outer RD - clearly bordered non-degenerated and degenerated outer retinal area - in all rabbits. We suggest our post-vitrectomy MNU-induced RD rabbit model could be used as an interim animal model for visual prosthetics before the transition to larger animal models.

**Key words:** Retinal degeneration, Intravitreal injection, N-methyl-N-nitrosourea, Vitrectomy, Optical coherence tomography, Animal model

## INTRODUCTION

Not only stem cell and gene therapy but also visual prosthetics such as retinal implants have been developed for the treatment of types of retinal degeneration (RD) like retinitis pigmentosa, choroideremia, and geographic atrophy of age-related macular degeneration [1-4]. Although some treatment modalities have shown positive results in vision restoration [1, 5-7], to further develop and

Received December 3, 2018, Revised February 1, 2019,  
Accepted February 7, 2019

\*To whom correspondence should be addressed.  
Yong Sook Goo, TEL: 82-43-261-2870, FAX: 82-43-272-1603  
e-mail: ysgoo@chungbuk.ac.kr  
Seong-Woo Kim, TEL: 82-2-2626-1260, FAX: 82-2-857-8580  
e-mail: ksw64723@korea.ac.kr

improve such treatment modalities, experimental larger animal models are inevitably needed, such as those involving pigs, cats, or rabbits exhibiting a selective loss of photoreceptors.

However, genetic models in larger animals are more difficult to establish and still have not been firmly developed yet, as compared with the state of rat and mouse models [8]. In animals larger than rats and mice, photoreceptor degeneration can also be induced by the systemic application of pharmaceuticals such as iodoacetic acid [9-11], sodium iodate (SI), or N-methyl-N-nitrosourea (MNU) [12-17]. However, intravenous or intraperitoneal administration can induce bilateral RD and systemic toxicity [18, 19]. MNU usage leads not only to bilateral RD but also to a downturn in the general health status of the experimental animals after systemic application. Besides short-term effects caused by the toxicity of the substance, the induction of tumors has been described as a long-term effect in rabbits and rats after systemic treatment with MNU [19], due to its DNA-alkylating mode of action. Therefore, considering animal welfare, limiting the blindness in one eye by direct drug application could be a good alternative to systemic application. Intravitreal injection to induce RD has been tried with various drugs in various kind of animals [20-27]. Rösch et al. determined that intravitreal application of MNU leads to unilateral photoreceptor degeneration in mice, thereby avoiding systemic side effects [20]. Separately, in pigmented rabbit eyes, intravitreal injection of MNU induced selective but inhomogeneous photoreceptor degeneration throughout the whole retina [26]. Retinal vascular structure is different depending on the species. Rabbit retinas are especially merangiotic and avascular, meaning that retinal vessels supply blood only a small part of the retina, extending in a horizontal direction to form bands on the optic disc. On the other hand, retinas in humans, primates, and dogs are holangiotic and vascular, meaning that the whole retina is vascularized by an intraretinal circulation scheme, involving for example the central retinal artery or cilioretinal arteries [28]. Although rabbit eyes are structurally different from those of larger animals or humans, a rabbit-focused experiment to establish an animal model of RD with intravitreal MNU injection could serve to develop and improve surgical procedures and implant techniques due to the similar size of rabbits' eyes with those of humans, prior to any transition to future investigations that use larger animals or humans.

Therefore, in the present study, first, we tried to find out whether vitrectomy affects the consistency of results in outer RD induced by intravitreal injection of MNU. Second, we sought to determine the optimal intravitreal dose of MNU to induce consistent outer RD in a rabbit model. Third, we attempted to identify outer RD induced by specific injection doses of intravitreal MNU with morphological and functional assay.

## MATERIALS AND METHODS

### Animals

In our dose-dependence study of MNU, the right eyes of male New Zealand white rabbits (n=38), each weighing between 2.5 kg and 3.5 kg, received either an intravitreal injection of MNU without vitrectomy or intravitreal injection of MNU or sham injection at two weeks after vitrectomy. For all MNU injections, each dose of MNU was diluted in 0.05 ml of phosphate-buffered saline (PBS). Intravitreal injection of MNU without vitrectomy was performed with the following different MNU concentrations; 0.4 mg, 0.3 mg, 0.2 mg, and 0.1 mg (n=4 rabbits per concentration for 0.4, 0.3, and 0.1 mg, n=7 rabbits for 0.2 mg), and 0.05 mg (n=2 rabbits). Intravitreal injection of MNU after vitrectomy was performed with the following: sham (0.05 ml of PBS, n=2 rabbits); 0.5 mg, 0.3 mg, 0.1 mg of MNU injection (n=4 rabbits per concentration) and 0.05 mg of MNU injection (n=3 rabbits). To identify morphological changes to the retina, ultra-wide-field color fundus photography (FP) and fundus autofluorescence (AF) imaging as well as spectral-domain optical coherence tomography (OCT) were performed at one month after intravitreal MNU injection. Histological examinations with hematoxylin and eosin (H&E) stain were also performed on selected rabbit eyes at one month after injection.

In our second study, based on the results of our dose-dependence study, 0.2 mg of MNU/0.05 ml was chosen for injection into the right eyes of rabbits (n=10) two weeks after vitrectomy. FP, AF imaging, OCT, and histology were then performed six weeks after injection. To identify physiological changes to the retina, electroretinography (ERG) of the retina was also performed at the same time.

All procedures adhered to the Association for Research in Vision and Ophthalmology (ARVO) Statement for the Use of Animals in Ophthalmic and Vision Research (ARVO Animal Policy). Approval for this study was obtained from the Institutional Animal Care and Use Committee of the Korea University College of Medicine in Seoul, Korea.

### Vitrectomy

The rabbits were anesthetized by an intravenous injection of alfaxalone (5 mg/kg; Alfaxan<sup>®</sup>, Jurox Pty Ltd., Rutherford, Australia) into the marginal auricular vein and intramuscular injection of xylazine (4 mg/kg; Rompun<sup>®</sup>, Bayer HealthCare Pharmaceuticals LLC, Berlin, Germany). After anesthesia, 0.5% tropicamide and 0.5% phenylephrine (Tropherine<sup>®</sup>; Hanmi Pharm, Seoul, Korea) were instilled into the eye for pupil dilatation and then the eye was irrigated with 5% povidone iodide and draped for surgery. Two-port 23-gauge core vitrectomy (Associate<sup>®</sup> system; Dutch

Ophthalmic Research Center, Zuidland, the Netherlands) was performed with a direct biconcave lens (Fig. 1). Two ports were prepared by inserting trocar cannulas into the sclera at a point 4 mm from the limbus at superoventral and superodorsal sides. Light was provided from a surgical microscope. The vitreous was removed using a vitreous cutter, while continually supplying a balanced salt solution (Alcon, Fort Worth, TX, USA).

#### ***Intravitreal injection of N-methyl-N-nitrosourea (MNU)***

Animals were anesthetized as described above. Immediately prior to the injections, MNU (Oakwood Products Inc., West Columbia, SC, USA) was dissolved in PBS. The right eye of each rabbit was prepared and the corresponding dose of MNU (with a volume of 0.05 ml) was injected intravitreally at a point 4 mm posterior to the limbus using a 30-gauge needle. No injections were performed in the left eyes.

#### ***Ultra-wide-field imaging and spectral-domain optical coherence tomography***

FP and fundus AF images were captured using an ultra-wide-field scanning laser ophthalmoscope (OPTOS 200 TX; Optos PLC, Dunfermline, UK). Spectral-domain OCT was performed using the Spectralis® OCT system (Heidelberg Engineering GmbH, Heidelberg, Germany). The area of the visual streak below the optic disc was evaluated. Vertical and horizontal line scans as well as raster scans (33 B-scans over a 16.5-mm×16.5-mm area in a 55-degree image) were performed in high-resolution mode (1536 A-scans per B-scan, lateral resolution=10 µm/pixel in a 55-degree image). Up to 100 single images were averaged using the automatic real-time mode to obtain a high-quality mean image. Retinal thickness was measured along a horizontal line perpendicular to

the retinal layers in cross-sectional images.

#### ***Electroretinography***

The ERG protocol was based on the international standard for electroretinography from the International Society for Clinical Electrophysiology of Vision (ISCEV). The rabbits were anesthetized as described above and dark-adapted for 30 minutes, after dark adaptation, the pupils were dilated. The light stimulation and ERG signal recordings were performed with a commercial system (RETIcom; Roland Consult, Brandenburg an der Havel, Germany), using a contact lens electrode with a built-in light resource (Kooijman/Damhof ERG lens; Medical Workshop BV, Groningen, the Netherlands). The reference and ground electrodes were platinum subdermal needle electrodes. Reference electrodes were placed in the skin near the lateral canthus of the eyes, and a ground electrode was placed on the forehead between the two eyes.

#### ***Histological examination***

Immediately after euthanasia, both eyes were enucleated and immersion-fixed in Davidson's solution for 24 hours, dehydrated, and then embedded in paraffin. Four-micrometer sections were subsequently cut and stained with H&E. The slides were examined to detect pathological changes in the retina using a light microscope (BX-53; Olympus Corp., Tokyo, Japan) and photographed with a digital video camera (INFINITY3-1UR; Lumenera Corp., Ottawa, ON, Canada).

#### ***Immunohistochemistry***

Tissue sections were deparaffinized, rehydrated, and microwave-heated in antigen retrieval buffer (1 mM of ethylenediaminetetraacetic acid (EDTA), 0.05% Tween 20, pH: 8.0). Sections were



**Fig. 1.** Photograph of a rabbit during the vitrectomy procedure. Two-port 23-gauge core vitrectomy was performed with a direct biconcave lens (a, b). Light was provided from a surgical microscope and the vitreous was removed using a vitreous cutter (b).

then blocked with 4% horse serum in PBS, followed by primary antibody incubation at 4°C overnight. For anti-PKCα (Invitrogen, Carlsbad, CA, USA) and Rhodamine labeled anti-PNA (Vector Laboratories, Burlingame, CA, USA) co-immunostaining, fluorescent detection was performed with Alexa Fluor 488–conjugated goat anti-mouse secondary antibodies (Invitrogen, Carlsbad, CA, USA). For anti-PKCα and anti-Rhodopsin (Rockland Immunochemicals, Pottstown, PA, USA) coimmunostaining, fluorescent detection was performed with Alexa Fluor 488–conjugated goat anti-mouse and Alexa Fluor 594–conjugated goat anti-mouse secondary antibodies (Invitrogen, Carlsbad, CA, USA). For anti-Brn3 (Santa Cruz Biotechnology, Dallas, TX, USA) immunostaining, fluorescent detection was performed with Alexa Fluor 594–conjugated goat anti-mouse secondary antibodies. For anti-GFAP (Novus Biological, Littleton, CO, USA) staining, sections were incubated for two hours at room temperature, then for one hour with Alexa Fluor 594–conjugated goat anti-mouse secondary antibodies. The deoxynucleotidyl transferase-mediated dUTP nick-end labeling (TUNEL) assay (Merck Millipore, Burlington, MA, USA)

was performed following the manufacturer’s protocol. Nuclei were counterstained with 4, 6-diamidino-2-phenylindole (DAPI) in the same sections (AnaSpec Inc., Fremont, CA, USA). Cells stained by TUNEL were evaluated using fluorescence microscopy (T2000-U; Nikon, Tokyo, Japan).

**Retinal thickness measurement and statistical analysis for retinal thinning induced by N-methyl-N-nitrosourea injection**

With OCT image, per each rabbit we measured total retinal thickness at eight different inferior retinal sites located 1 disc apart from visual streak and normalized retinal thinning was calculated as [(retinal thickness after injection)–(retinal thickness before injection)]/(retinal thickness before injection). Three out of ten rabbits which were injected with 0.2 mg MNU after vitrectomy, cataracts were found during the examination performed at six weeks after injection. Therefore, we excluded these 3 rabbits from the data pool. Only seven rabbits with vitrectomy were used for retinal thickness comparison.

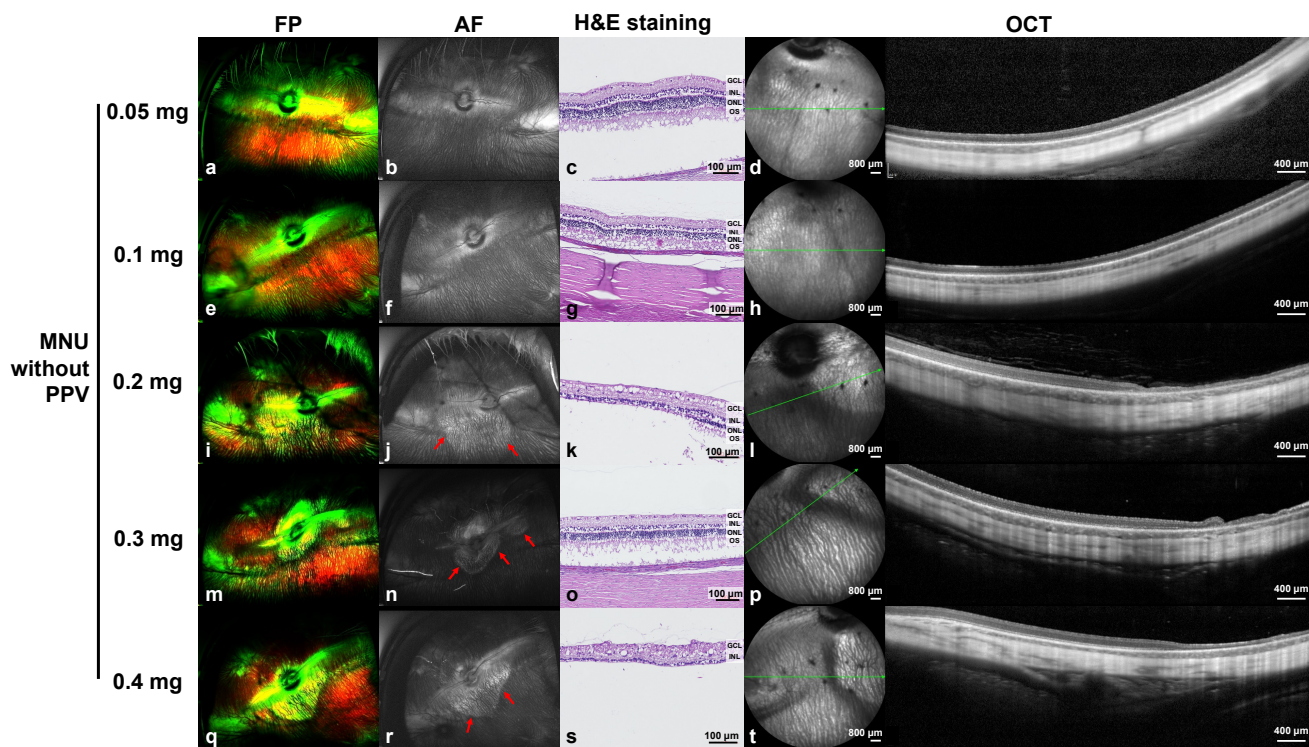


**Fig. 2.** Ultra-wide-field color FP, AF, histology with H&E staining, and OCT images at one month after intravitreal injection of MNU without vitrectomy. One month after injection, no significant changes were observed in the FP, AF, histology, and OCT images of rabbit eyes with either 0.05 mg (a–d) or 0.1 mg (e–h) of injected MNU. Focal geographic hyper-AF areas (red arrows) were observed in the cases of 0.2 mg (j), 0.3 mg (n), and 0.4 mg (r) MNU injections. More severe retinal atrophy as seen in the photograph with H&E staining and OCT was induced via the 0.2 mg (k, l) and 0.4 mg (s, t) MNU injections versus with the 0.3 mg MNU injection (o, p). The green line on infrared FP shows the plane where the OCT image was harvested. Each scale bar on H&E staining (c, g, k, o, and s), infrared FP (left side image of d, h, l, p, and t), and OCT (right side image of d, h, l, p, and t) represents 100 μm, 800 μm, and 400 μm, respectively.

To compare the effect of MNU injection on retinal thickness between non-vitrectomy and vitrectomy group, statistical analysis was conducted by Student's t-test. Data are represented as mean±standard deviation (SD). The differences were considered statistically significant at  $p < 0.05$ .

## RESULTS

### *Imaging of retina in dose-dependence study of N-methyl-N-nitrosourea without pars plana vitrectomy*

One month after intravitreal MNU injection without vitrectomy, no changes in the retina were observed with the lower doses of MNU (i.e., 0.05 mg and 0.1 mg) (Fig. 2a~2h). Focal RD was noted, however, with the 0.2 mg, 0.3 mg, and 0.4 mg injections of MNU (Fig. 2i~2t). However, in contrast to our expectations, more severe and broad retinal atrophy was induced with an injection of 0.2 mg of MNU (Fig. 2i~2l) than with one of 0.3 mg of MNU (Fig. 2m~2p).

### *Imaging of retina in dose-dependence study of N-methyl-N-nitrosourea after pars plana vitrectomy*

One month after MNU injection in the vitrectomized eyes, ultra-wide-field imaging of the retina was performed. Localized geographic hyper-AF areas with strong linear hyper-AF borders were noted with 0.3 mg and 0.5 mg of MNU injection in eyes after vitrectomy (Fig. 3n and 3r). No changes in the retina were observed in the sham-injected and lower MNU doses (0.05 mg and 0.1 mg)-injected eyes after vitrectomy (Fig. 3b, 3f, and 3j).

No significant retinal changes were observed via OCT, in the sham- and 0.05 and 0.1 mg of MNU-injected eyes after vitrectomy (Fig. 3d, 3h, and 3l). However, in the retina of 0.5 mg MNU-injected eyes, whole retinal layer thinning was noticed in the degenerated area of the retina, while, on OCT imaging of the normal area of the retina, such looked intact (Fig. 3t). Severe outer RD was induced in all four rabbit eyes injected with 0.3 mg of MNU following injection (Fig. 3p). Histological examination using H&E staining is presented in Fig. 3. In eyes that received 0.5 mg of MNU, whole retinal layer thinning was observed in the degenerated area

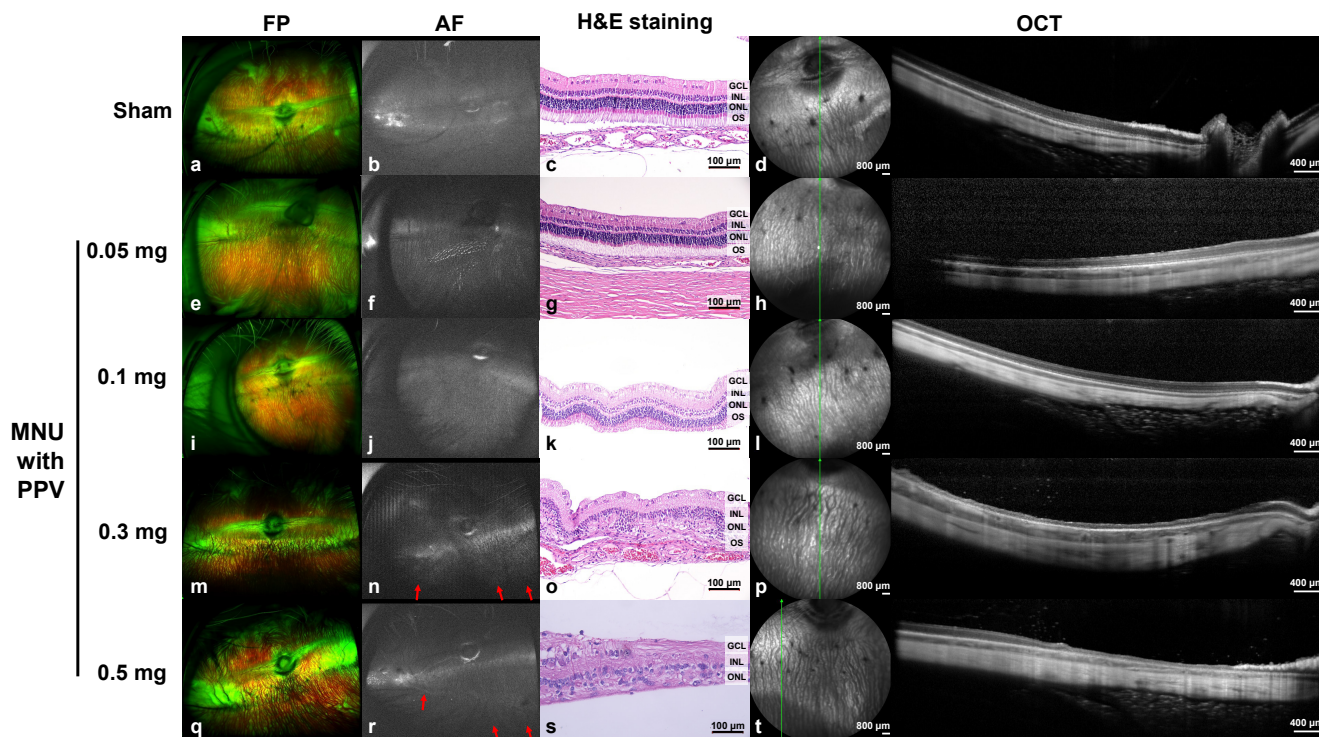


**Fig. 3.** Ultra-wide-field color FP and AF, spectral-domain OCT, and H&E staining images at one month after intravitreal MNU injection with pars plana vitrectomy. At one month after injection, no significant changes were observed in the FP, AF, OCT and H&E staining images of the rabbit eyes that received sham (a~d) or 0.05 mg (e~h) or 0.1 mg (i~l) of MNU injections after vitrectomy. Localized geographic hyper-AF areas with linear hyper-AF borders (red arrows) were observed with the 0.3 mg (n) and 0.5 mg (r) MNU injections after vitrectomy. Additionally, degenerative changes to the retina in OCT were observed in 0.3 mg (p) and 0.5 mg (t) MNU injections after vitrectomy. Loss of the photoreceptor layer and disruption of the layers of the retina were observed via H&E staining at the degeneration region with OCT (o, s). The green line on infrared FP shows the plane where the OCT image was harvested. Each scale bar on H&E staining (c, g, k, o, and s), infrared FP (left side image of d, h, l, p, and t), and OCT (right side image of d, h, l, p, and t) represents 100  $\mu$ m, 800  $\mu$ m, and 400  $\mu$ m, respectively.

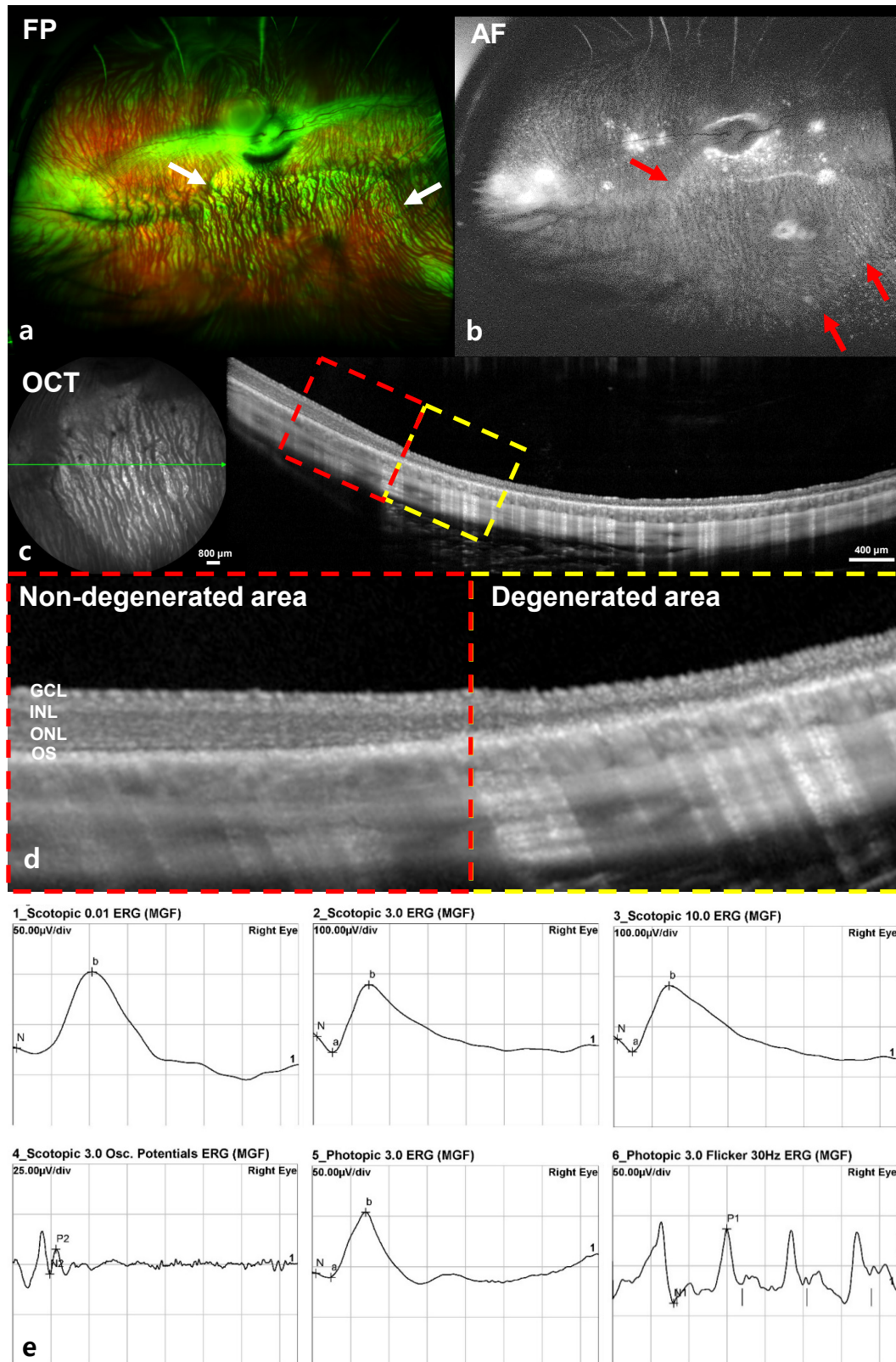


**Fig. 4.** Ultra-wide-field color FP, AF, spectral-domain OCT, and ERG images at six weeks after MNU (0.2 mg) injection with vitrectomy. Hyper-AF in the AF image (red arrow) and significant retinal changes in OCT at hyper-AF lesions were found (a~d). In the magnified OCT image (d, dashed-line box in Figure 4c), the borderline between the degenerated area and non-degenerated area was clearly delineated and the degeneration of the outer retina and retinal thinning were detected in the degenerated area (d, yellow dashed-line box). ERG responses were normal (e).

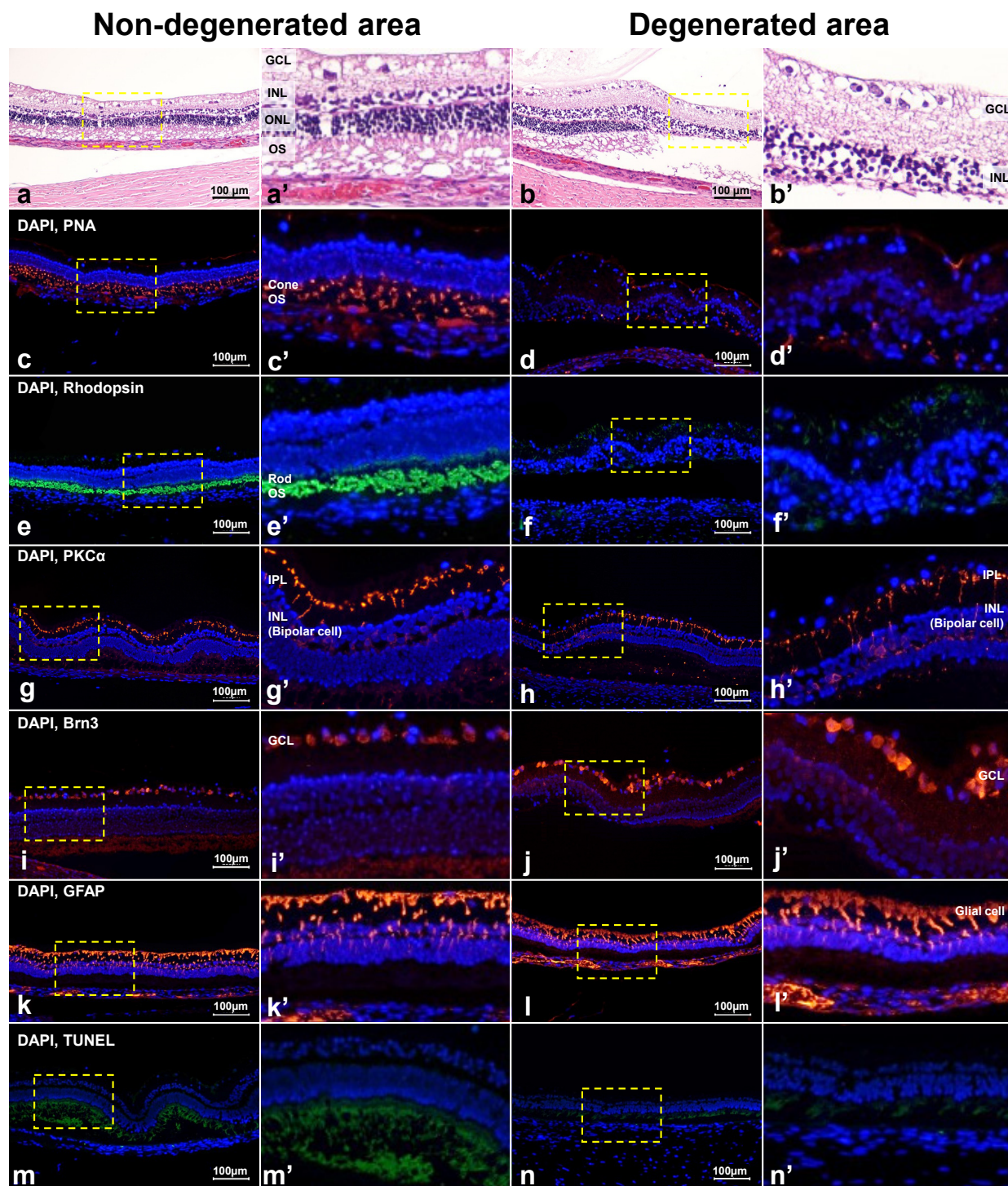


**Fig. 5.** The difference in histology with H&E staining and immunohistochemistry with PNA, Rhodopsin, PKC $\alpha$ , Brn3, GFAP, and TUNEL assay between the non-degenerated and degenerated areas at six weeks after intravitreal injection of 0.2 mg of MNU with vitrectomy. Histology with H&E staining showed not only the photoreceptor layer but also all layers of the retina appeared normal in the non-degenerated area (a), but loss of the photoreceptor layer was found in the degenerated area (b). In the non-degenerated area, cone and rod photoreceptor cells were normally expressed with PNA (c) and Rhodopsin staining (e), respectively. However, in the degenerated area, the cone photoreceptor cells were less expressed with PNA staining (d) and the rod photoreceptor cells were less expressed with Rhodopsin staining (f). Bipolar cells were well-expressed with PKC $\alpha$  staining (g, h) and ganglion cells were well-expressed with Brn3 staining (i, j) in both the non-degenerated (g, i) and degenerated areas (h, j) of the retina. Both the non-degenerated and degenerated areas showed an increase in GFAP staining (k, l), and there were no TUNEL-positive cells in either area (m, n). Next to all figures, three times enlarged figures (the part of dashed yellow box of a~n) are shown (a'~n').

of the retina (Fig. 3s). Additionally, eyes injected with 0.3 mg of MNU showed a loss of the photoreceptor layer (Fig. 3o).

**Localized retinal degeneration induced by a 0.2 mg N-methyl-N-nitrosourea injection with vitrectomy**

Based on our dose-dependence study, 0.2 mg/0.05 ml of MNU was chosen for further investigation. Six weeks after a 0.2 mg MNU injection, outer RD had developed in all of 10 rabbits.

All 10 rabbits showed hyper-AF with or without a linear hyper-AF border in the AF image and significant retinal changes in OCT in the hyper-AF lesion (Fig. 4a~4d). The disruption of the outer retina and retinal thinning were detected in the degenerated area. All of the degenerated retinal area was predominantly localized on the inferior retina within a measurement of one-disc diameter from the optic disc, and about two-thirds of inferior retina was degenerated. All the ERG responses were within the normal range despite the localized degeneration (Fig. 4e).

The non-degenerated and degenerated areas showed a difference

upon histological examination (Fig. 5). In the non-degenerated area, H&E stain showed normal retinal structure (Fig. 5a) and peanut agglutinin (PNA), Rhodopsin, PKC $\alpha$ , and Brn3 staining showed intact retinal cells, which were cone photoreceptors, rod photoreceptors, bipolar cells, and ganglion cells, respectively (Fig. 5c, 5e, 5g, and 5i). However, in the degenerated area, H&E staining showed that the outer retina layer was disrupted (Fig. 5b); cone and rod photoreceptors were also decreased according to PNA and Rhodopsin staining (Fig. 5d and 5f). However, bipolar cells and ganglion cells were still intact according to PKC $\alpha$  and Brn3 staining in the degenerated area (Fig. 5h and 5j). Both non-degenerated and degenerated areas showed an increase in GFAP staining (Fig. 5k and 5l), and there were no TUNEL-positive cells in either case (Fig. 5m and 5n).

**Quantitative comparison of N-methyl-N-nitrosourea injection between non-vitrectomy and vitrectomy group**

We compared dose-dependence effect of MNU between non-

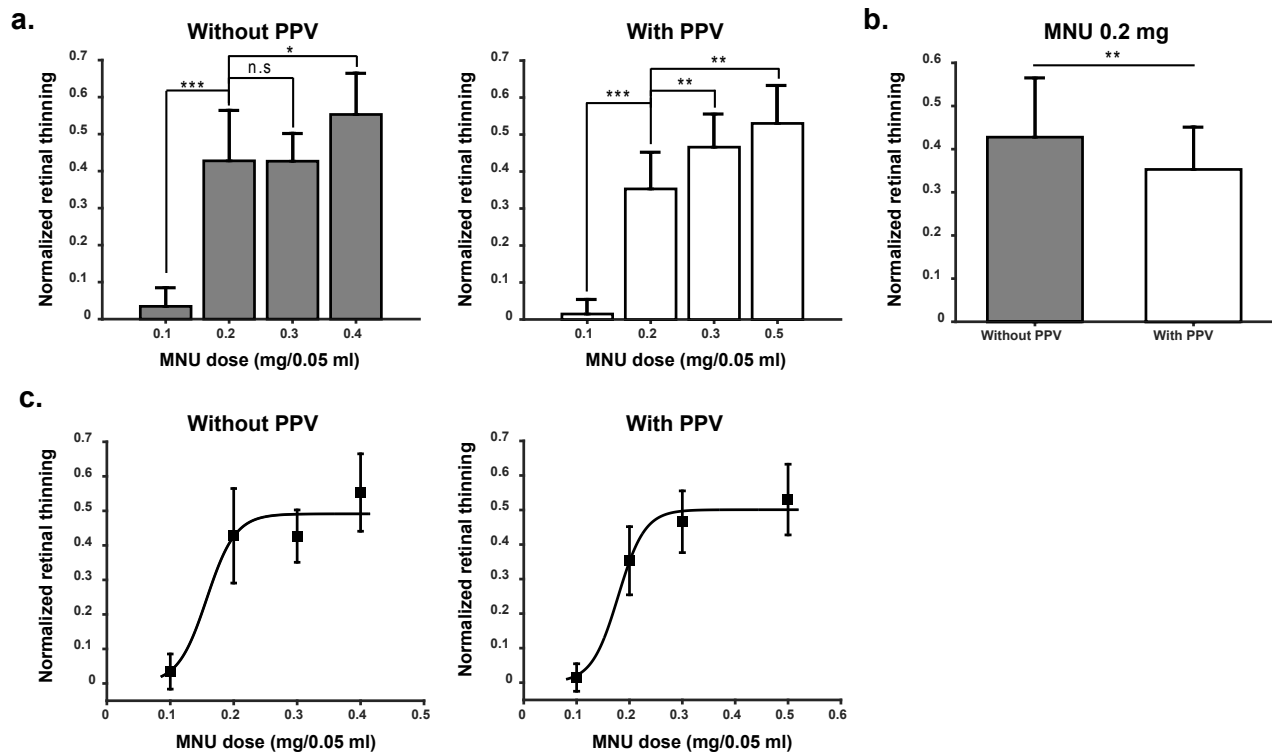


**Fig. 6.** Comparison of MNU injection between non-vitrectomy and vitrectomy group. Both without pars plana vitrectomy (PPV) group and with PPV group, 4 rabbits per each MNU dose were used. The exception was found with 0.2 mg MNU injection, 7 rabbits for each PPV group and non-PPV group, respectively. (a) Without vitrectomy group, 0.2 mg MNU induced significantly more retinal thinning than 0.1 mg (\*\* $p < 0.001$ ) but there was no difference between 0.2 mg and 0.3 mg injection (not significant (n.s):  $p > 0.05$ ). With vitrectomy group, 0.2 mg MNU induced significantly different retinal thinning with all other doses (0.1 mg, 0.3 mg, and 0.5 mg). (b) Comparison of 0.2 mg MNU injection between non-PPV group and PPV group. In non-PPV group ( $n = 7$ ), significantly more retinal thinning was induced than that in PPV group (\*\* $p < 0.01$ ). The standard deviation (S.D.) was smaller in vitrectomy group than non-vitrectomy group. (c) From the data of A, curve fitting was performed, and sigmoidal curve fit provides the best  $R^2$  value ( $R^2 = 0.99$ ) in vitrectomy group. Mean and S.D. was shown in each figure. Student-t test was performed for statistical analysis.



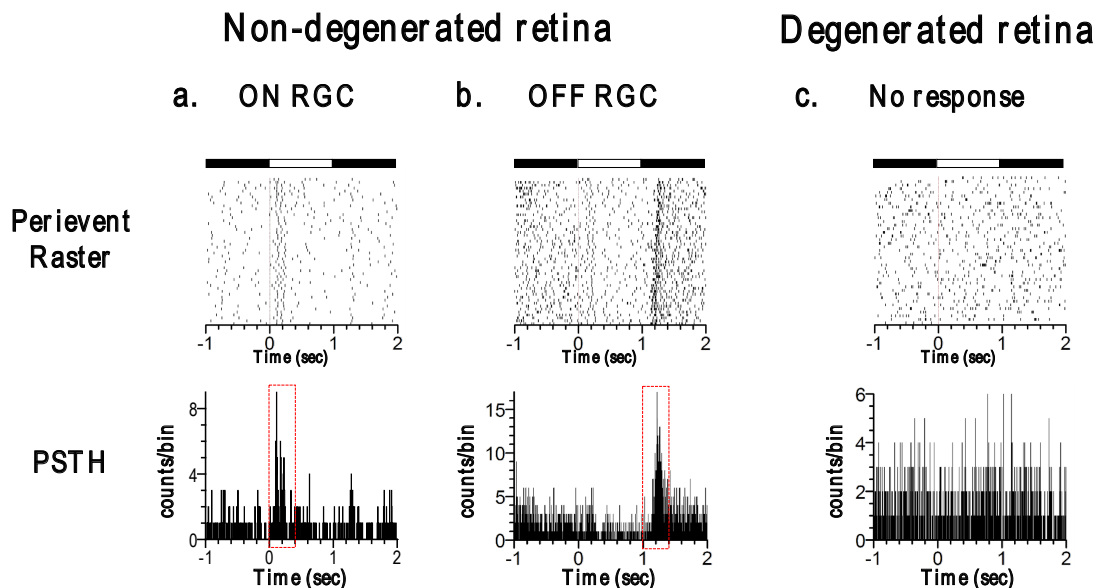


**Fig. 7.** Light-evoked RGC responses in non- and degenerated retinal areas. (a) ON RGC response of non-degenerated retinal area stimulated with full-field illumination ( $40 \mu\text{W}/\text{cm}^2$  intensity), top: peri-event raster plot (ON: 1 s, OFF: 2 s, 30 trials), bottom: post-stimulus time histogram (PSTH) constructed from 30 trials (bin: 5 ms). (b) OFF RGC response of non-degenerated retinal area. (c) No light responses in degenerated retinal area.

vitrectomy and vitrectomy group (Fig. 6). With vitrectomy, retinal thinning induced by 0.2 mg MNU injection showed significant difference among all other doses (0.1 mg, 0.3 mg, and 0.5 mg) and dose-dependence curve was very well fitted with sigmoid curve (goodness of fit  $R^2=0.99$ ; Fig. 6c right). On the contrary, without vitrectomy, there was no difference in retinal thinning between 0.2 mg and 0.3 mg injection ( $p>0.05$ ; Fig. 6a). Therefore, the dose-dependence curve was not well fitted (Fig. 6c left). In comparison of 0.2 mg injection between non-vitrectomy ( $n=7$  rabbits) and vitrectomy ( $n=7$  rabbits), non-vitrectomy rabbits showed more retinal thinning than vitrectomy rabbits (Mean $\pm$ S.D.;  $0.43\pm 0.14$  vs.  $0.35\pm 0.10$ ;  $p<0.01$ ; Fig. 6b). The possible explanation of this difference will be discussed in discussion section.

#### **Light-evoked RGC responses in non-degenerated and degenerated retinal patches**

We recorded light-evoked responses both in degenerated and non-degenerated retinal areas using a multichannel recording system (Fig. 7). All of the details on how to prepare an ex-vivo retinal patch and multichannel recording system have been described in our previous papers [29-32]. With full-field illumination of a rabbit retinal patch mounted on a multielectrode array, light-evoked retinal ganglion cell (RGC) responses were well-categorized as ON-cell and OFF-cell in the non-degenerated retinal area (Fig. 7a and 7b). However, in the degenerated retinal area, there was no light-evoked response (Fig. 7c).

#### **DISCUSSION**

In this study, localized outer RD was consistently induced only with intravitreal injection of MNU after vitrectomy. Without vitrectomy, the degree of RD was unpredictable and dose-independent. From the initial dose-dependence study investigating MNU dose, an MNU dose of 0.2 mg/0.05 ml was chosen as optimal and an injection of this amount was shown to induce localized outer RD in all rabbits ( $n=10$ ). We identified and confirmed the localized outer RD with morphological assay.

#### **Morphological identification of retinal degeneration induced by N-methyl-N-nitrosourea injection**

In this study, we used ultra-wide FP and AF imaging to evaluate whether the induced RD was global or localized (focal). Localized hyper-AF changes were detected in all wide-field fundus images (Fig. 4b). Because every outer RD zone was located around the optic disc, 55-degree OCT and its infrared image locating the inferior disc margin of the rabbit retina at the 12 o'clock direction of the image border could successfully detect the retinal degeneration zone. Intravitreal MNU injection-induced outer RD and the change in the retina found via OCT was confirmed through histological examination with immunohistochemistry in this study (Fig. 5). GFAP staining shows expression at the end feet of Müller cells and expression increases in retinal injury or inflammatory conditions, therefore, GFAP is a representative marker for retinal

injury or stress [33]. In our study, GFAP staining was increased in both the non-degenerated and degenerated areas in the ganglion cell, inner plexiform, and inner nuclear layers, and it seems that the performance of vitrectomy and intravitreal injection caused retinal stress and induced fibrosis and proliferation of glial cells, regardless of degeneration [34].

#### ***Physiological identification of retinal degeneration induced by N-methyl-N-nitrosourea injection***

The ERGs of albino rabbits presented significantly larger amplitudes in scotopic, photopic, and flicker responses compared to those of pigmented rabbits. This finding might be attributed to the greater availability of light due to scatter and reflection at the retinal layer in albino rabbits [35]. Rösch et al. reported that a complete loss of ERG potentials was observed in two of three pigmented rabbits after an MNU injection of 3 mg/kg body weight (BW) [26]. On the contrary, in this study, the ERGs of 0.2 mg of MNU injected–white rabbit eyes presented no significantly abnormal findings. There was intact retinal area in the sectoral geographic degeneration type and the normal response to light was possibly evoked from that intact part of the retina. Therefore, our scotopic and photopic ERGs showed normal waveforms (Fig. 4e). In a future study, we will use multifocal ERG recording to show focal retinal changes in response to light.

To confirm selective photoreceptor layer loss in our 0.2 mg MNU–induced RD model, we recorded light-evoked responses both in degenerated and non-degenerated retinal areas using a multichannel recording system (Fig. 7). Our ex-vivo functional study with multielectrode array clearly showed that in the degenerated retinal area, there was no light-evoked response (Fig. 7c), which represents strong evidence for the functional loss of photoreceptors.

#### ***Advantage of intravitreal injection of N-methyl-N-nitrosourea with vitrectomy***

Subretinal injection can also be used to induce a focal RD model [36, 37]. However, it is difficult to insert the cannula near the optic disc or visual streak, and subretinal injection induces focal degeneration as well, as the eyeball is a closed organ and permits very a narrow degree of intraocular pressure change without vitrectomy. On the other hand, the localized application of MNU through intravitreal injection after vitrectomy has advantages. First, it spares the untreated eye and avoids unwanted systemic side-effects. Second, when the vitrectomy is performed, intravitreal injection induces relatively wider localized RD compared to subretinal injection. Third, it is easier to do research on the effects of intravitreal injection in any kind of animal model.

The difference between our research and Rösch et al's [26] study was the effects of vitrectomy on MNU-induced RD. Although they tried hard to control the dose-dependent MNU effect by using MNU doses from 1 mg to 6 mg/BW, without vitrectomy, they never succeeded in inducing consistent changes among different rabbits. The injection of 3 mg/kg BW of MNU only induced selective photoreceptor degeneration. However, even with an MNU injection of 3 mg/kg BW, the degree of degeneration varied between different parts of the same retina and between the retinas of different animals. Based on their study, it seems that the degree of RD could not be controlled by injected MNU dose without vitrectomy and that RD was induced in a very restricted retinal area. In our study, by performing pars plana vitrectomy prior to intravitreal MNU injection, we could induce dose-dependent–localized outer RD with solid reproducibility and a relatively large-sized (about two-thirds of the inferior retina)–localized outer RD (Fig. 6). We also analyzed the degree of localized degenerative change through ultra-wide-field color FP, AF, and OCT images without sacrifice of the animal. Therefore, we can recognize how diffuse and wide the localized degenerative area in the retina is after intravitreal injection. About two-thirds of the inferior retina was degenerated in all our cases. With vitrectomy, the vitreous, which might act as a diffusion barrier, was eliminated and the unreliable diffusion of MNU might have been decreased; therefore, a quite consistent degree of outer RD was induced [38, 39]. Our result shows that 0.2 mg MNU injection in non-vitrectomy rabbits induced significantly more retinal thinning than that in vitrectomy rabbits (Fig. 6b). Due to unreliable diffusion of MNU, MNU may be very focally localized in non-vitrectomy rabbits. Therefore, when we measured the retinal thickness, this poor diffusion may affect the percentile change of retinal thickness in non-vitrectomy group. While in vitrectomy group, RD was induced reliably in a dose-dependent way (Fig. 6c) and MNU injection induced a consistent degree of outer RD than non-vitrectomy group (smaller S.D. in Fig. 6b).

Among 10 eyes of 10 rabbits after 0.2 mg/0.05 ml of MNU injection, cataracts caused by instrumental lens touch occurred in three out of the 10 eyes of 10 rabbits (30.0%) during vitrectomy and were found during the examination performed at six weeks after injection. Although the cataracts were brought on unintentionally, the shapes of the cataracts were in a wedge pattern, meaning that they were caused by vitrectomy rather than MNU toxicity. Moreover, signs of systemic toxicity such as weight loss or death were not found in any of our rabbits. Therefore, these findings showed the safety of the localized administration by intravitreal injection with MNU.

### **Possible mechanism of N-methyl-N-nitrosourea for inducing retinal degeneration**

MNU is an alkylating agent that targets photoreceptor cells and interacts with DNA to yield a variety of reaction products [15]. It has been reported that MNU induces the accumulation of intracellular calcium ions in the retina and induces calpain-dependent photoreceptor cell loss following intraperitoneal injection [40]. MNU leads to extensive oxidative stress in a dose-dependent manner, resulting in retinal photoreceptor degeneration. Although the mechanism of MNU-induced photoreceptor cell loss is not fully understood, an animal model with MNU-induced RD through intravitreal injection after vitrectomy can be widely useful as an RD model for the investigation of visual prosthetics or other treatment studies.

### **ACKNOWLEDGEMENTS**

This research was supported in part by the Basic Science Research Program through the National Research Foundation of Korea (NRF), funded by the Ministry of Education (NRF-2016R1D1A1A02937018) and the Bio & Medical Technology Development Program of the NRF funded in part by the Ministry of Science and ICT (MSIP) (NRF-2017M3A9E2056458 and 2017M3A9E2056460).

### **REFERENCES**

1. da Cruz L, Coley BF, Dorn J, Merlini F, Filley E, Christopher P, Chen FK, Wuyyuru V, Sahel J, Stanga P, Humayun M, Greenberg RJ, Dagnelie G, Argus II; Argus II Study Group (2013) The Argus II epiretinal prosthesis system allows letter and word reading and long-term function in patients with profound vision loss. *Br J Ophthalmol* 97:632-636.
2. Humayun MS, Weiland JD, Fujii GY, Greenberg R, Williamson R, Little J, Mech B, Cimmarusti V, Van Boemel G, Dagnelie G, de Juan E Jr (2003) Visual perception in a blind subject with a chronic microelectronic retinal prosthesis. *Vision Res* 43:2573-2581.
3. MacLaren RE, Pearson RA, MacNeil A, Douglas RH, Salt TE, Akimoto M, Swaroop A, Sowden JC, Ali RR (2006) Retinal repair by transplantation of photoreceptor precursors. *Nature* 444:203-207.
4. Sahni JN, Angi M, Irigoyen C, Semeraro F, Romano MR, Parmeggiani F (2011) Therapeutic challenges to retinitis pigmentosa: from neuroprotection to gene therapy. *Curr Genomics* 12:276-284.
5. Finn AP, Grewal DS, Vajzovic L (2018) Argus II retinal prosthesis system: a review of patient selection criteria, surgical considerations, and post-operative outcomes. *Clin Ophthalmol* 12:1089-1097.
6. Gekeler K, Bartz-Schmidt KU, Sachs H, MacLaren RE, Stingl K, Zrenner E, Gekeler F (2018) Implantation, removal and replacement of subretinal electronic implants for restoration of vision in patients with retinitis pigmentosa. *Curr Opin Ophthalmol* 29:239-247.
7. Stingl K, Bartz-Schmidt KU, Besch D, Chee CK, Cottrill CL, Gekeler F, Groppe M, Jackson TL, MacLaren RE, Koitschev A, Kusnyerik A, Neffendorf J, Nemeth J, Naem MA, Peters T, Ramsden JD, Sachs H, Simpson A, Singh MS, Wilhelm B, Wong D, Zrenner E (2015) Subretinal Visual Implant Alpha IMS--Clinical trial interim report. *Vision Res* 111:149-160.
8. Tso MO, Li WW, Zhang C, Lam TT, Hao Y, Petters RM, Wong F (1997) A pathologic study of degeneration of the rod and cone populations of the rhodopsin Pro347Leu transgenic pigs. *Trans Am Ophthalmol Soc* 95:467-479.
9. Liang L, Katagiri Y, Franco LM, Yamauchi Y, Enzmann V, Kaplan HJ, Sandell JH (2008) Long-term cellular and regional specificity of the photoreceptor toxin, iodoacetic acid (IAA), in the rabbit retina. *Vis Neurosci* 25:167-177.
10. Noell WK (1953) Experimentally induced toxic effects on structure and function of visual cells and pigment epithelium. *Am J Ophthalmol* 36:103-116.
11. Scott PA, Kaplan HJ, Sandell JH (2011) Anatomical evidence of photoreceptor degeneration induced by iodoacetic acid in the porcine eye. *Exp Eye Res* 93:513-527.
12. Herrold KM (1967) Pigmentary degeneration of the retina induced by N-methyl-N-nitrosourea. An experimental study in syrian hamsters. *Arch Ophthalmol* 78:650-653.
13. Nagar S, Krishnamoorthy V, Cherukuri P, Jain V, Dhingra NK (2009) Early remodeling in an inducible animal model of retinal degeneration. *Neuroscience* 160:517-529.
14. Nambu H, Yuge K, Nakajima M, Shikata N, Takahashi K, Miki H, Uyama M, Tsubura A (1997) Morphologic characteristics of N-methyl-N-nitrosourea-induced retinal degeneration in C57BL mice. *Pathol Int* 47:377-383.
15. Tsubura A, Yoshizawa K, Kuwata M, Uehara N (2010) Animal models for retinitis pigmentosa induced by MNU; disease progression, mechanisms and therapeutic trials. *Histol Histopathol* 25:933-944.
16. Tsuruma K, Yamauchi M, Inokuchi Y, Sugitani S, Shimazawa M, Hara H (2012) Role of oxidative stress in retinal photoreceptor cell death in N-methyl-N-nitrosourea-treated mice. *J Pharmacol Sci* 118:351-362.
17. Yoshizawa K, Yang J, Senzaki H, Uemura Y, Kiyozuka Y, Shika-

- ta N, Oishi Y, Miki H, Tsubura A (2000) Caspase-3 inhibitor rescues N-methyl-N-nitrosourea-induced retinal degeneration in Sprague-Dawley rats. *Exp Eye Res* 71:629-635.
18. McCormick DL, Rao KV, Dooley L, Steele VE, Lubet RA, Kelloff GJ, Bosland MC (1998) Influence of N-methyl-N-nitrosourea, testosterone, and N-(4-hydroxyphenyl)-all-trans-retinamide on prostate cancer induction in Wistar-Unilever rats. *Cancer Res* 58:3282-3288.
  19. Schreiber D, Jänisch W, Warzok R, Tausch H (1969) [Induction of brain and spinal cord tumors in rabbits with N-methyl-N-nitrosourea]. *Z Gesamte Exp Med* 150:76-86.
  20. Rösch S, Johnen S, Mataruga A, Müller F, Pfarrer C, Walter P (2014) Selective photoreceptor degeneration by intravitreal injection of N-methyl-N-nitrosourea. *Invest Ophthalmol Vis Sci* 55:1711-1723.
  21. Aplin FP, Fletcher EL, Luu CD, Vessey KA, Allen PJ, Guymer RH, Shepherd RK, Shivdasani MN (2016) Stimulation of a suprachoroidal retinal prosthesis drives cortical responses in a feline model of retinal degeneration. *Invest Ophthalmol Vis Sci* 57:5216-5229.
  22. Aplin FP, Luu CD, Vessey KA, Guymer RH, Shepherd RK, Fletcher EL (2014) ATP-induced photoreceptor death in a feline model of retinal degeneration. *Invest Ophthalmol Vis Sci* 55:8319-8329.
  23. Aplin FP, Vessey KA, Luu CD, Guymer RH, Shepherd RK, Fletcher EL (2016) Retinal Changes in an ATP-Induced Model of Retinal Degeneration. *Front Neuroanat* 10:46.
  24. Cho BJ, Seo JM, Yu HG, Chung H (2016) Monocular retinal degeneration induced by intravitreal injection of sodium iodate in rabbit eyes. *Jpn J Ophthalmol* 60:226-237.
  25. Halupka KJ, Abbott CJ, Wong YT, Cloherty SL, Grayden DB, Burkitt AN, Sergeev EN, Luu CD, Brandli A, Allen PJ, Meffin H, Shivdasani MN (2017) Neural responses to multielectrode stimulation of healthy and degenerate retina. *Invest Ophthalmol Vis Sci* 58:3770-3784.
  26. Rösch S, Werner C, Müller F, Walter P (2017) Photoreceptor degeneration by intravitreal injection of N-methyl-N-nitrosourea (MNU) in rabbits: a pilot study. *Graefes Arch Clin Exp Ophthalmol* 255:317-331.
  27. Vessey KA, Greferath U, Aplin FP, Jobling AI, Phipps JA, Ho T, De Iongh RU, Fletcher EL (2014) Adenosine triphosphate-induced photoreceptor death and retinal remodeling in rats. *J Comp Neurol* 522:2928-2950.
  28. Lossi L, D'Angelo L, De Girolamo P, Merighi A (2016) Anatomical features for an adequate choice of experimental animal model in biomedicine: II. Small laboratory rodents, rabbit, and pig. *Ann Anat* 204:11-28.
  29. Ahn KN, Ahn JY, Kim JH, Cho K, Koo KI, Senok SS, Goo YS (2015) Effect of stimulus waveform of biphasic current pulse on retinal ganglion cell responses in retinal degeneration (rd1) mice. *Korean J Physiol Pharmacol* 19:167-175.
  30. Goo YS, Ahn KN, Song YJ, Ahn SH, Han SK, Ryu SB, Kim KH (2011) Spontaneous oscillatory rhythm in retinal activities of two retinal degeneration (rd1 and rd10) mice. *Korean J Physiol Pharmacol* 15:415-422.
  31. Goo YS, Ye JH, Lee S, Nam Y, Ryu SB, Kim KH (2011) Retinal ganglion cell responses to voltage and current stimulation in wild-type and rd1 mouse retinas. *J Neural Eng* 8:035003.
  32. Goo YS, Park DJ, Ahn JR, Senok SS (2015) Spontaneous oscillatory rhythms in the degenerating mouse retina modulate retinal ganglion cell responses to electrical stimulation. *Front Cell Neurosci* 9:512.
  33. Chang SW, Kim HI, Kim GH, Park SJ, Kim IB (2016) Increased expression of osteopontin in retinal degeneration induced by blue light-emitting diode exposure in mice. *Front Mol Neurosci* 9:58.
  34. Ulbricht E, Pannicke T, Uhlmann S, Wiedemann P, Reichenbach A, Francke M (2013) Activation of retinal microglial cells is not associated with Muller cell reactivity in vitrectomized rabbit eyes. *Acta Ophthalmol* 91:e48-55.
  35. Ioshimoto GL, Camargo AA, Liber AM P, Nagy BV, Damico FM, Ventura DF (2018) Comparison between albino and pigmented rabbit ERGs. *Doc Ophthalmol* 136:113-123.
  36. Liu C, Cao L, Yang S, Xu L, Liu P, Wang F, Xu D (2015) Subretinal injection of amyloid- $\beta$  peptide accelerates RPE cell senescence and retinal degeneration. *Int J Mol Med* 35:169-176.
  37. Lyzogubov VV, Bora NS, Tytarenko RG, Bora PS (2014) Polyethylene glycol induced mouse model of retinal degeneration. *Exp Eye Res* 127:143-152.
  38. Reichenbach A, Schnitzer J, Friedrich A, Ziegert W, Brückner G, Schober W (1991) Development of the rabbit retina. I. Size of eye and retina, and postnatal cell proliferation. *Anat Embryol (Berl)* 183:287-297.
  39. Williams D (2007) Rabbit and rodent ophthalmology. *EJCAP* 17:242-252.
  40. Oka T, Nakajima T, Tamada Y, Shearer TR, Azuma M (2007) Contribution of calpains to photoreceptor cell death in N-methyl-N-nitrosourea-treated rats. *Exp Neurol* 204:39-48.